

Chapman University
Chapman University Digital Commons

Education Faculty Articles and Research

College of Educational Studies

8-24-2016

Quantifying Peat Carbon Accumulation in Alaska Using a Process-Based Biogeochemistry Model

Sirui Wang

Purdue University

Qianlai Zhuang

Purdue University

Zicheng Yu

Lehigh University


Scott Bridgham

University of Oregon

Jason K. Keller

Chapman University, jkeller@chapman.edu

Follow this and additional works at: http://digitalcommons.chapman.edu/education_articles

 Part of the [Biogeochemistry Commons](#), [Hydrology Commons](#), [Other Earth Sciences Commons](#), and the [Soil Science Commons](#)

Recommended Citation

Wang, S., Q. Zhuang, Z. Yu, S. Bridgham, and J. K. Keller (2016), Quantifying peat carbon accumulation in Alaska using a process-based biogeochemistry model, *J. Geophys. Res. Biogeosci.*, 121, 2172–2185, doi:10.1002/2016JG003452.

This Article is brought to you for free and open access by the College of Educational Studies at Chapman University Digital Commons. It has been accepted for inclusion in Education Faculty Articles and Research by an authorized administrator of Chapman University Digital Commons. For more information, please contact laughtin@chapman.edu.

Quantifying Peat Carbon Accumulation in Alaska Using a Process-Based Biogeochemistry Model

Comments

This article was originally published in *Journal of Geophysical Research: Biogeosciences*, volume 121, in 2016.
DOI: [10.1002/2016JG003452](https://doi.org/10.1002/2016JG003452)

Copyright

American Geophysical Union

RESEARCH ARTICLE

10.1002/2016JG003452

Key Points:

- We develop a model coupling hydrology, soil thermal, methane, ecosystem carbon, and nitrogen to quantify long-term peat carbon accumulation
- We compare modeled soil moisture and temperature, water table, methane, and carbon pools with observation and apply the model to Alaskan peatland
- High summer temperature from elevated insolation seasonality and high precipitation may be main factor for rapid carbon accumulation

Supporting Information:

- Supporting Information S1

Correspondence to:

Q. Zhuang,
qzhuang@purdue.edu

Citation:

Wang, S., Q. Zhuang, Z. Yu, S. Bridgman, and J. K. Keller (2016), Quantifying peat carbon accumulation in Alaska using a process-based biogeochemistry model, *J. Geophys. Res. Biogeosci.*, 121, 2172–2185, doi:10.1002/2016JG003452.

Received 12 APR 2016

Accepted 29 JUL 2016

Accepted article online 4 AUG 2016

Published online 24 AUG 2016

Quantifying peat carbon accumulation in Alaska using a process-based biogeochemistry model

Sirui Wang¹, Qianlai Zhuang^{1,2}, Zicheng Yu³, Scott Bridgman⁴, and Jason K. Keller⁵

¹Department of Earth, Atmospheric, and Planetary Sciences, Purdue University, West Lafayette, Indiana, USA, ²Department of Agronomy, Purdue University, West Lafayette, Indiana, USA, ³Department of Earth and Environmental Sciences, Lehigh University, Bethlehem, Pennsylvania, USA, ⁴The Institute of Ecology and Evolution, University of Oregon, Eugene, Oregon, USA, ⁵Schmid College of Science and Technology, Chapman University, Orange, California, USA

Abstract This study uses an integrated modeling framework that couples the dynamics of hydrology, soil thermal regime, and ecosystem carbon and nitrogen to quantify the long-term peat carbon accumulation in Alaska during the Holocene. Modeled hydrology, soil thermal regime, carbon pools and fluxes, and methane emissions are evaluated using observation data at several peatland sites in Minnesota, Alaska, and Canada. The model is then applied for a 10,000 year (15 ka to 5 ka; 1 ka = 1000 cal years before present) simulation at four peatland sites. We find that model simulations match the observed carbon accumulation rates at ten sites during the Holocene ($R^2 = 0.88, 0.87, 0.38,$ and -0.05 using comparisons in 500 year bins). The simulated (2.04 m) and observed peat depths (on average 1.98 m) were also compared well ($R^2 = 0.91$). The early Holocene carbon accumulation rates, especially during the Holocene thermal maximum (HTM) ($35.9 \text{ g C m}^{-2} \text{ yr}^{-1}$), are estimated up to 6 times higher than the rest of the Holocene ($6.5 \text{ g C m}^{-2} \text{ yr}^{-1}$). Our analysis suggests that high summer temperature and the lengthened growing season resulted from the elevated insolation seasonality, along with wetter-than-before conditions might be major factors causing the rapid carbon accumulation in Alaska during the HTM. Our sensitivity tests indicate that, apart from climate, initial water table depth and vegetation canopy are major drivers to the estimated peat carbon accumulation. When the modeling framework is evaluated for various peatland types in the Arctic, it can quantify peatland carbon accumulation at regional scales.

1. Introduction

The Arctic has experienced significant warming in the twentieth century, and this warming is predicted to continue in this century [*Arctic Climate Impact Assessment*, 2005]. Terrestrial ecosystems in this region occupy a large portion (22%) of the global land surface with approximately 40% of global land carbon [*McGuire et al.*, 1995; *McGuire and Hobbie*, 1997]. The ongoing and future warming is expected to change the cycling of carbon stored in these ecosystems, leading to either a negative or a positive feedback to the global climate system [*Davidson and Janssens*, 2006; *Christensen and Christensen*, 2007; *Jones and Yu*, 2010].

Northern peatlands store 200–600 Pg (1 Pg = 10^{15} g) carbon depending on depth considered [*Gorham*, 1991; *Turunen et al.*, 2002; *McGuire et al.*, 2009; *Yu et al.*, 2010], which accounts for up to one third of the world's soil carbon [*Post et al.*, 1982; *Gorham*, 1991]. They are mainly located in Russia, Canada, United States, and Fennoscandian countries [*Lappalainen*, 1996; *Turunen et al.*, 2002]. A number of studies have quantified the climate impact on carbon dynamics in peatlands [e.g., *Kirschbaum*, 1993, 1995; *Wang and Polglase*, 1995; *Deng et al.*, 2015; *Zhuang et al.*, 2015; *Knorr et al.*, 2005], but no consensus on the net effect of climate change on peat carbon accumulation has been reached. A number of soil core analyses and modeling indicate that warming reduces soil organic carbon storage [e.g., *Kirschbaum*, 2000, 2006; *Davidson and Janssens*, 2006; *Gerdol et al.*, 2008], but others suggest that there is an acceleration of soil carbon sequestration [*Yu et al.*, 2009; *Jones and Yu*, 2010].

Many existing studies on peatland carbon dynamics are based on short-term observation and model simulations [e.g., *Turetsky et al.*, 2008, 2014; *Bridgman et al.*, 2008; *Deng et al.*, 2015]. These short-term analyses may not be adequate for understanding the response of peat carbon to long-term climate change. To overcome this, peat core data have been used to infer the peat carbon accumulation rates during the Holocene in various regions [e.g., *Turunen et al.*, 2002; *Roulet et al.*, 2007; *Gorham et al.*, 2003; *Yu et al.*, 2009]. Most long-term observational studies have focused on individual sites, but recently, some large-scale syntheses have been carried out [*Yu et al.*, 2010; *Loisel et al.*, 2014]. Models are another means of examining long-term response to climate

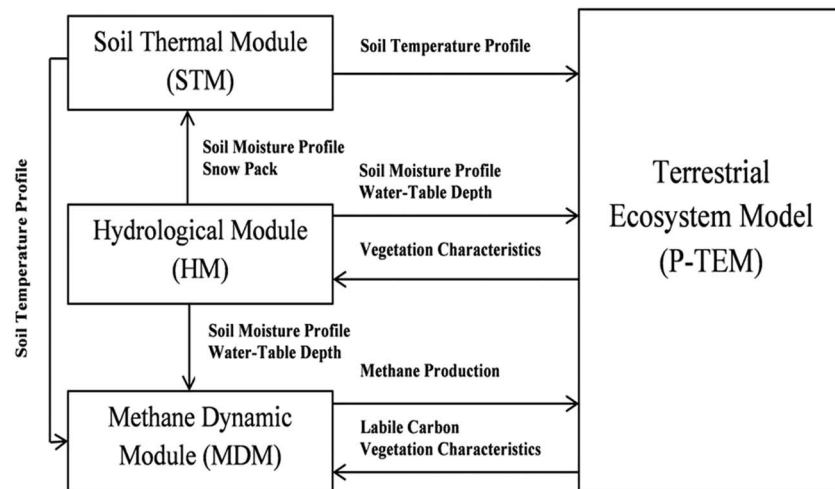


Figure 1. P-TEM modeling framework includes a soil thermal module (STM), a hydrologic module (HM), a carbon/nitrogen dynamic model (TEM), and a methane dynamic module (MDM) [Zhuang *et al.*, 2002, 2004, 2006].

change. Spahni *et al.* [2013] imbedded a peatland module into a dynamic global vegetation and land surface process model (LPX-Bern 1.0) and conducted a transient simulation of carbon dynamics in northern peatlands from the Last Glacial Maximum to the 21st century. Frolking *et al.* [2010] also modeled the peat carbon accumulation rate and peat depth profile for an 8000 year old ombrotrophic bog (Mer Bleue) in Canada. However, these models have not explicitly considered the effects of permafrost dynamics or were based on a simple algorithm to model soil temperature effects on peat carbon dynamics. Further, some of these models have not considered the nitrogen feedback to the carbon cycling in nitrogen-limited northern peatlands.

In the past few decades, peat core data have been collected in the circum-Arctic region [Yu *et al.*, 2009]. Fluxes of carbon, water, and energy in peatland ecosystems in the region have also been measured [Turetsky *et al.*, 2008; Churchill, 2011]. However, existing peatland modeling studies have not taken advantage of these rich data. Here we develop and evaluate a peatland biogeochemistry model (P-TEM) based on an extant biogeochemistry model, the Terrestrial Ecosystem Model (TEM) [Zhuang *et al.*, 2003; 2004]. The model explicitly considers the effects of permafrost and hydrological dynamics as well as nitrogen feedback to the carbon cycling of peatland ecosystems. The model is then used to examine peat carbon accumulation rates for Alaskan peatlands during the Holocene.

2. Methods

2.1. Overview

We first develop the P-TEM by coupling and revising a core carbon and nitrogen dynamic module (CNDM) of TEM [Zhuang *et al.*, 2003], the soil thermal module (STM) [Zhuang *et al.*, 2001], the methane dynamic module (MDM) [Zhuang *et al.*, 2004, 2006], and a hydrological module (HM) [Zhuang *et al.*, 2002] (Figure 1). Second, we evaluate hydrological dynamics using observed data of soil moisture and water table depth at peatland sites in Alaska and Canada. We evaluate soil temperature estimates using data collected in Alaskan peatlands. We also evaluate methane emission estimates using methane flux data of a peatland in Minnesota. Third, we apply the model to four peatlands sites on the Kenai Peninsula, Alaska, driven with paleoclimate data from ECBilt-CLIO (The Earth System Model of Intermediate Complexity) model output [Timm and Timmermann, 2007] to evaluate peat carbon accumulation rate and depth profile by comparing to peat core data. Finally, we test the model sensitivity to various controls and factors as a way to identify the main factors that influence peat carbon dynamics.

2.2. Model Modification

Peat soil organic carbon (SOC) accumulation is determined by the net primary production (NPP) and aerobic and anaerobic respiration. Peatlands accumulate carbon where NPP is greater than decomposition, resulting in positive net ecosystem production (NEP). The core carbon and nitrogen dynamic module of TEM was developed for upland ecosystems [Zhuang *et al.*, 2003], where NEP is calculated at a monthly time step:

Table 1. Variables and Model Parameters Used for Calculating Heterotrophic Respiration in This Study

Variables	Description	Unit
R_H	Monthly heterotrophic respiration of soil organic carbon (upland soils)	$\text{g C m}^{-2} \text{ month}^{-1}$
R'_H	Monthly aerobic heterotrophic respiration of soil organic carbon (peatland soils)	$\text{g C m}^{-2} \text{ month}^{-1}$
R_{CH_4}	Monthly methane emission	$\text{g C m}^{-2} \text{ month}^{-1}$
R_{CWM}	Monthly CO_2 emission due to methane oxidation	$\text{g C m}^{-2} \text{ month}^{-1}$
R_{CM}	Monthly CO_2 emission due to methanogenesis	$\text{g C m}^{-2} \text{ month}^{-1}$
R_{COM}	Monthly CO_2 emission due to other anaerobic processes	$\text{g C m}^{-2} \text{ month}^{-1}$
K_d	Logarithm of heterotrophic respiration rate at 0°C	$\text{g C g}^{-1} \text{ mol}^{-1}$
C_5	Quantity of the state variable describing total amount of soil organic carbon (SOC)	g C m^{-2}
C_{50}	SOC between the lowest water table boundary and soil surface (equilibrium)	g C m^{-2}
C_{51}	SOC between the lowest water table boundary and soil surface (transient)	g C m^{-2}
M_V	Soil water content (upland soils)	%
M'_V	Soil water content in the unsaturated zone (peatland soils)	%
H_T	Mean monthly temperature of the organic soil layer	$^\circ\text{C}$
LWB	Lowest water table boundary (fixed model parameter)	mm
WTD	Water table depth	mm

$$\text{NEP} = \text{NPP} - R_H \quad (1)$$

SOC heterotrophic respiration (R_H) is calculated as (Table 1):

$$R_H = K_d C_5 f(M_V) e^{0.069H_T} \quad (2)$$

where $f(M_V)$ is a nonlinear relationship that describes the effect of soil moisture in the unsaturated zone on microbial activity for decomposition. Soil moisture affects oxygen level in soils. K_d is the logarithm of heterotrophic respiration rate at 0°C . C_5 is the total amount of upland mineral SOC above the plant rooting depth. H_T is the mean monthly temperature of the organic layer.

Here we revise the decomposition to include both aerobic heterotrophic respiration above the water table, which produces CO_2 , and anaerobic respiration below water table, which produces both CO_2 and methane (CH_4). The soil organic carbon accumulation rate (ΔSOC) is equal to NEP, where NEP is calculated as

$$\text{NEP} = \text{NPP} - R'_H - R_{\text{CH}_4} - R_{\text{CWM}} - R_{\text{CM}} - R_{\text{COM}} \quad (3)$$

R_{CH_4} represents the monthly methane emission after methane oxidation, and R_{CWM} represents the CO_2 emission due to methane oxidation [Zhuang *et al.*, 2015]. A ratio of 1:1 is assumed to calculate the CO_2 release (R_{CM}) accompanied with the methanogenesis [Tang *et al.*, 2010; Conrad, 1999]. R_{COM} represents the CO_2 release from other anaerobic processes (e.g., fermentation and terminal electron acceptor reduction) [Keller and Bridgman, 2007; Keller and Takagi, 2013]. The ratio of $R_{\text{COM}} : R_{\text{CH}_4}$ varies largely according to previous studies. The molar ratios ($\text{CO}_2 : \text{CH}_4$) of the emission rates under inundated conditions were 4–173 for the fen and bog, respectively [Moore and Knowles, 1989], while Freeman *et al.* [1992] and Yavitt *et al.* [1987] estimated this ratio as 1. Here we assume $R_{\text{COM}} : R_{\text{CH}_4}$ to be 5 so that the simulated $\text{CO}_2 : \text{CH}_4$ of the emission rates from the anaerobic processes is ~ 10 for a fen (see Discussion). R'_H now represents the monthly aerobic respiration related to the variability of water table depth (WTD; Table 1):

$$R'_H = K_d C_{51} f(M'_V) e^{0.069H_T} \times \frac{\text{WTD}}{\text{LWB}} \quad (4)$$

where M'_V represents the soil water content in the unsaturated zone above the WTD. The SOC between the lowest water table boundary (LWB; a fixed model parameter, the soil below which is set saturated; see Table 1) and soil surface (C_{51}) in the transient condition is obtained after a 2000 year equilibrium run.

We model peatland soils as a two-layer system (Table S2 in the supporting information) based on the three-layer system for upland (Table S1) in the hydrological module (HM). The soil layers above the LWB are divided into 1 cm sublayers, where peat soil characteristics in the upper peat are constant above 7 cm peat depth and changed linearly in the section interval of 1 cm below (Table S2) [Granberg *et al.*, 1999; Zhuang *et al.*, 2004]. P_{tot} is the total porosity (Table S2) and is set to 0.98 below the WTD. The actual WTD is estimated based on the total amount of water content above the LWB within upper two boxes. Using the calculated WTD, the water content at each 1 cm above the water table can be then determined after solving the water balance equations.

Table 2. Sites Used for Parameterization for Hydrological Module (HM), Methane Dynamic Module (MDM), and Soil Thermal Module (STM)

Site	Description	Vegetation	Simulation Period	Observed Variables for HM (or MDM) Parameterization	Observed Variables for STM Parameterization
Saskatchewan (SK) 1977 Fire	Evergreen broadleaf forest site in Saskatchewan, Canada. Mean annual temperature is 0.4°C, with mean total precipitation 467.2 mm (1971–2000 Wasikesiu normals)	Jack pine black spruce	Jan 2004 to Dec 2005	VSM at 30 cm	Soil temperature at depths of 10 cm, 20 cm, and 50 cm
Delta Junction 1920 Control	Evergreen needleleaf forest located near Delta Junction, to the north of the Alaska Range in Interior Alaska [Serikowsky, 2001]	Evergreen needleleaf forest	Jan 2002 to Dec 2003	VSM at 4 cm, 11 cm, and 37 cm	Soil temperature at depths of 10 cm and 20 cm
Delta Junction 1999 Burn	Located near Delta Junction, to the north of the Alaska Range in Interior Alaska, within 15 km of Delta Junction 1920 Control. The 70% of the area is not covered by vascular plants, with mean annual temperature -2.3°C , annual accumulated rainfall 304 mm, and snowfall 940 mm	Open tundra with black spruce (<i>Picea mariana</i>) and bunch grasses (<i>Festuca altaica</i> ; 30%)	Jan 2002 to Dec 2003	VSM at depths of 4 cm and 11 cm	-
APEXCON	Lowland open fen along Bonanza Creek Road at the base of the bluff, Bonanza Creek, Interior Alaska. The area is classified as continental boreal with a mean annual temperature of -2.9°C and annual accumulated precipitation of 269 mm, of which 30% is snow [Hinzman et al., 2006]	Moderate rich open fen with sedges (<i>Carex</i> sp.), spiked rushes (<i>Eleocharis</i> sp.), <i>Sphagnum</i> spp., and brown mosses (<i>Drepanocladus aduncus</i>)	Growing season in 2007 and from 2009 to 2011	Water table depth and methane emission	Soil temperature at depths of 10 cm, 25 cm, and 50 cm
SPRUCE	Bog forest in northern Minnesota, 40 km of Grand Rapids in the USDA Forest Service Marcell Experimental Forest (MEF). Mean annual temperature from 1961 to 2005 is 3.3°C ; annual accumulated precipitation is 768 mm, with 75% of it occurring in the snow-free period from mid-April to early November [Crill et al., 1988]	<i>Picea mariana</i> - <i>Sphagnum</i> spp. bog	Growing season from 2011 to 2014	Water table depth and methane emissions	-

Table 3. Sites Used for Comparison of Carbon Accumulation Rates Between Simulation and Observation [Jones and Yu, 2010]

Site Name	Location	Peatland Type	Latitude	Longitude	Dating Method	No. of Dates	Basal Age (cal years B.P.)	Time-Weighted Holocene Accumulation Rates (g C m ⁻² yr ⁻¹)
Kenai Gasfield	Alaska, USA	fen	60°27'N	151°14'W	AMS	12	11,408	13.1
No Name Creek	Alaska, USA	fen	60°38'N	151°04'W	AMS	11	11,526	12.3
Horsetrail fen	Alaska, USA	rich fen	60°25'N	150°54'W	AMS	10	13,614	10.7
Swanson fen	Alaska, USA	poor fen	60°47'N	150°49'W	AMS	9	14,225	5.7

In the STM module, the soil vertical profile is divided into four layers: (1) snowpack in winter, (2) moss (or litter) layer, (3) organic soil (upper organic layer and lower organic layer for peatland soils), and (4) mineral soil. The mineral layer is set to be water saturated for peatland soils (Table S3). Each of these soil layers is characterized with a distinct soil thermal conductivity and heat capacity. The observed soil water content data are used to drive STM.

The methane dynamic module (MDM) [Zhuang *et al.*, 2004] explicitly considers the process of methane production (methanogenesis); methane oxidation (methanotrophy); and the transportation pathways including (1) diffusion through the soil profile, (2) plant-aided transportation, and (3) ebullition. Methane oxidation is simulated as an aerobic process that occurs only in the unsaturated zone. Hourly methanotrophy is estimated within each 1 cm layer. The MDM gets the soil temperature inputs calculated from STM. HM estimated the WTD and soil water content in the unsaturated zone affects methane production and emission. Net primary production (NPP) is calculated from the CNDM. Soil-water pH is prescribed from the site-observed data, and the root distribution determines the redox potential.

2.3. Model Evaluation

We evaluate the modeling framework with respect to hydrological dynamics, peat soil thermal dynamics, and carbon and methane dynamics using observed data at various peatland sites. We first evaluate the modeled volumetric soil moisture (percent) at three upland sites in Alaska (Delta Junction 1920 and 1999) and Canada (SK 1977; Table 2). The forcing climate data include air temperature, precipitation, global incoming solar radiation or photosynthetically active radiation, and water vapor pressure. The water vapor pressure is obtained from the calculation of observed air temperature at canopy height and relative humidity. The snow rate is obtained by equally splitting the total annual accumulated snowfall into months during the winter. Second, we evaluate the simulated water table depth and methane emissions at APEXCON and SPRUCE sites (Table 2). The APEXCON site, characterized as a lowland open fen, is located outside the boundaries of the Bonanza Creek Experimental Forest. The APEXCON site is a moderate rich fen with mean pH of 5.3, which lacks trees and is dominated by a diverse community of emergent aquatic plants (*Carex* and *Equisetum*), brown moss, and *Sphagnum* with the thickness of peat approximately 1 m. The weekly observed methane fluxes using static chambers during the growing seasons are for the period of 2005–2011. Hourly water table depth was continuously recorded from June to October each year. The SPRUCE site is characterized as a *Picea mariana* (black spruce)-*Sphagnum* spp. bog forest. The 0.5 h observed meteorological data [Hanson *et al.*, 2015], water table depth, and methane flux data during the growing seasons from 2011 to 2014 [Iversen *et al.*, 2014; Hanson *et al.*, 2014] were aggregated to a monthly time step for model input.

Third, we evaluate the simulated soil temperature profile using observed data at Saskatchewan 1977 Fire and Delta Junction 1920 sites for upland soils and APEXCON for peatland soils. We also evaluate the simulated carbon dynamics of a fen at the APEXCON site.

2.4. Model Application

We apply P-TEM to four peatlands on the Kenai Peninsula, Alaska (Table 3) [Jones and Yu, 2010; Yu *et al.*, 2009]. The observed data include the peat depth, percentage of organic matter, and bulk density of both organic and inorganic matter at 1 cm intervals. The percentage of organic matter in the peat sample and the bulk density are used to convert the simulated peat carbon to the total peat depth profile. The ratio of the peat SOC over peat organic matter is set to be 0.468 from the soil carbon amount distribution database [Loisel *et al.*, 2014].

In the simulation, we assume that the initial waterlogging event occurred 2000 years before peat starts to form, which provides the necessary hydrological conditions for peatland formation. We run the model for 2000 years

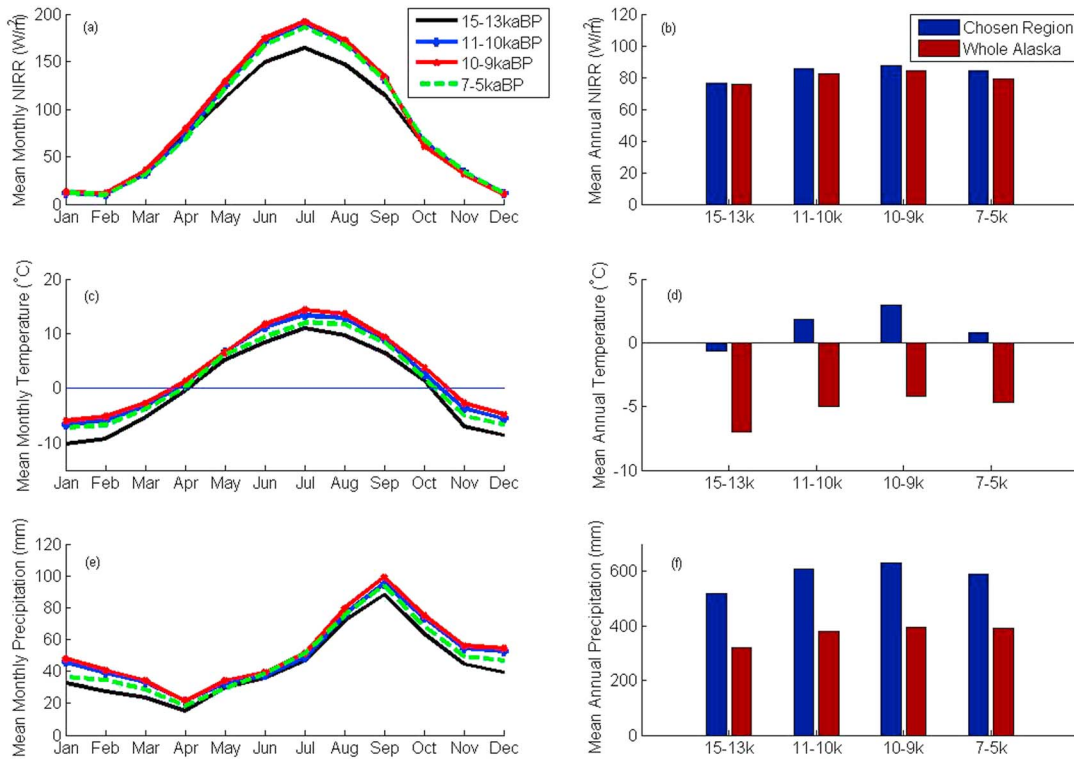


Figure 2. Climate data output from the paleoclimate simulations during the postglacial period (15–13, 11–10, 10–9, and 7–5 ka): (a) mean monthly and (b) mean annual net incoming solar radiation (NIRR) of the whole of Alaska and the chosen pixels, (c) mean monthly and (d) mean annual temperature of the whole of Alaska and the chosen pixels, and (e) mean monthly and (f) mean annual precipitation of the whole of Alaska and the chosen pixels.

to reach equilibrium to get the initial soil carbon C_{50} . The transient simulation starts after reaching the equilibrium as C_{50} no longer changes, providing a stable soil carbon amount from the LWB to the soil surface at 15 ka.

The accumulation of peat carbon is examined at four time slices including a time slice encompassing a millennial-scale warming event during the last deglaciation known as the Bølling-Allerød at 15–13 ka, the Holocene thermal maximum (HTM) during the early Holocene at 11–10 and 10–9 ka, and the mid-Holocene at 7–5 ka B.P. The climate data in two time periods, from 13 to 11 ka and from 9 to 7 ka, were not explicitly simulated, but we used the linear interpolation from adjacent slices and filled these two missing slices. Climate data were downscaled, and bias was corrected from ECBilt-CLIO model output [Timm and Timmermann, 2007; He et al., 2014]. Climate fields include monthly precipitation, monthly air temperature, monthly net incoming solar radiation (NIRR; Figure 2), and monthly vapor pressure ($2.5^\circ \times 2.5^\circ$). The ECBilt-CLIO model has been used in other HTM studies, where the model produced the interaction between orbital-induced summer insolation and ice sheet configuration that were reflected in proxy records [Renssen et al., 2009]. We apply delta-ratio bias correction with observed half-degree data from the Climate Research Unit version 2.0 and the inverse-square distance interpolation method, similar to the approach taken to downscale and bias-correct future climate scenarios [Hay et al., 2000], to correct the climate anomalies for the detailed topography and coastlines of northern high latitudes at a resolution of $0.5^\circ \times 0.5^\circ$. To drive the P-TEM, we use the same time-dependent forcing atmospheric carbon dioxide concentration data as were used in ECBilt-CLIO transient simulations from the Taylor Dome [Timm and Timmermann, 2007].

We also conduct a sensitivity analysis for peat carbon accumulation in response to variations of the lowest water table boundary (LWB) and the leaf area index (LAI). In the “standard” simulation, the LWB is set to 30 cm below the soil surface, while in the “more saturated” and “less saturated” scenarios, it is set to 22 cm and 38 cm, respectively. We conduct the test with other variables remaining unchanged. As the water table position is raised, less space will be available for the microbial aerobic respiration, leading to an increasing amount of methane production, and vice versa. We are interested in estimating the long-term influence of different LWB on the simulation of peatland carbon accumulation in P-TEM.

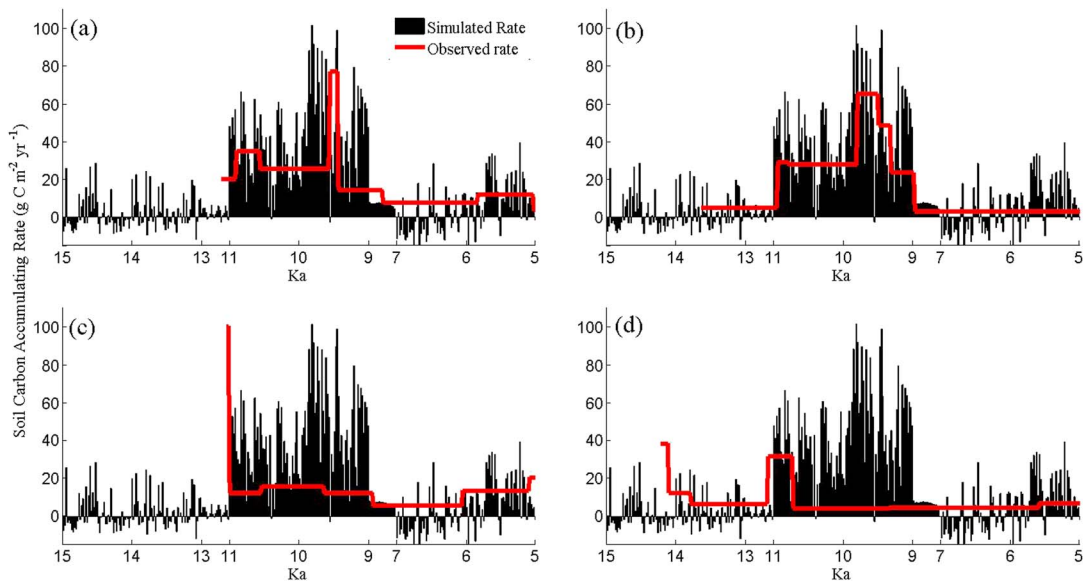


Figure 3. Simulated and observed carbon accumulation rates from 15 ka to 5 ka. The red solid lines represent the observed time-weighted rates for (a) No Name Creek, (b) Horse Trail Fen, (c) Kenai Gasfield, and (d) Swanson Fen. The black solid lines represent the simulated averaged carbon accumulation rate of every 20 years.

Leaf area index (LAI) defines the leaf area for snow and rain interception by the vegetation canopy. Different values of LAI lead to different hydrological conditions. We conduct three simulations: the forested peatland with the LAI set to 5.0 [Coughlan and Running, 1997] and the maximum daily canopy interception of rain ($I_{R\max}$) (Table S1) set to 0.26 [Helvey, 1971; Zhuang et al., 2002] through the year, a partly forested peatland with LAI 2.8 and $I_{R\max}$ set to 0.1, and an open peatland with LAI set to 0.4 and $I_{R\max}$ set to 0.0. The standard simulation is the open fen, and we also conduct simulations for two other vegetation types to investigate how the different LAI can influence the interception of monthly precipitation and thus cause the change of peat carbon accumulation.

3. Results and Discussion

3.1. Model Evaluation

Based on the adjusted parameters for upland (Table S1) and peatland (Table S2) in the HM, the result of the shallowest layer of soils in Delta Junction 1999 and 1920 suggests that the HM can accurately simulate the soil moisture content in both open tundra and boreal forest ($R^2 = 0.94$ and 0.76 for Delta Junction 1920 and 1999, respectively; Figures S1a and S1b in the supporting information). Especially during the growing season, the water content is much higher at the tundra site, suggesting a higher rainfall through the plant canopy due to the smaller leaf interception area (Figure S1e). Similarly, HM has the capacity to simulate the soil moisture content for the deeper layer ($R^2 = 0.92$ and 0.83 for SK 1977 Fire and Delta Junction 1920, respectively; Figures S1c and S1d). The HM well simulates the monthly water table depth at both APEXCON and SPRUCE sites ($R^2 = 0.92$ and 0.52 , respectively; Figure S2).

Based on the adjusted parameters in the STM (Table S3), the model reproduces the soil temperature profile with R^2 values of 0.94, 0.96, and 0.67 at 10 cm, 20 cm, and 50 cm, respectively, at the SK 1977 Fire site (Figure S3). Similarly, compared with observations, the model captures the soil temperature for the Delta Junction 1920 site with R^2 values 0.83 and 0.85 at 10 cm and 20 cm and for the APEXCON site with R^2 values of 0.96, 0.92, and 0.81 at 10 cm, 25 cm, and 50 cm, respectively (Figure S3). Furthermore, the MDM-estimated methane fluxes match observations with R^2 values of 0.90 and 0.40 for the two sites after incorporating the calculated soil moisture in the unsaturated zone, water table depth, and soil temperature profile from other modules (Figure S4).

Based on the adjusted parameters in the CNDM, the simulated annual fluxes and pools of carbon and nitrogen are within the range of the observations at APEXCON in 2009 and other references (Table S4).

3.2. Peatland Carbon Accumulation

P-TEM simulations for the six grid cells in Kenai Peninsula show a large variation from 15 ka to 5 ka, ranging from a peat carbon loss to peat carbon gain of $100 \text{ g C m}^{-2} \text{ yr}^{-1}$ on average (Figure 3). The most obvious

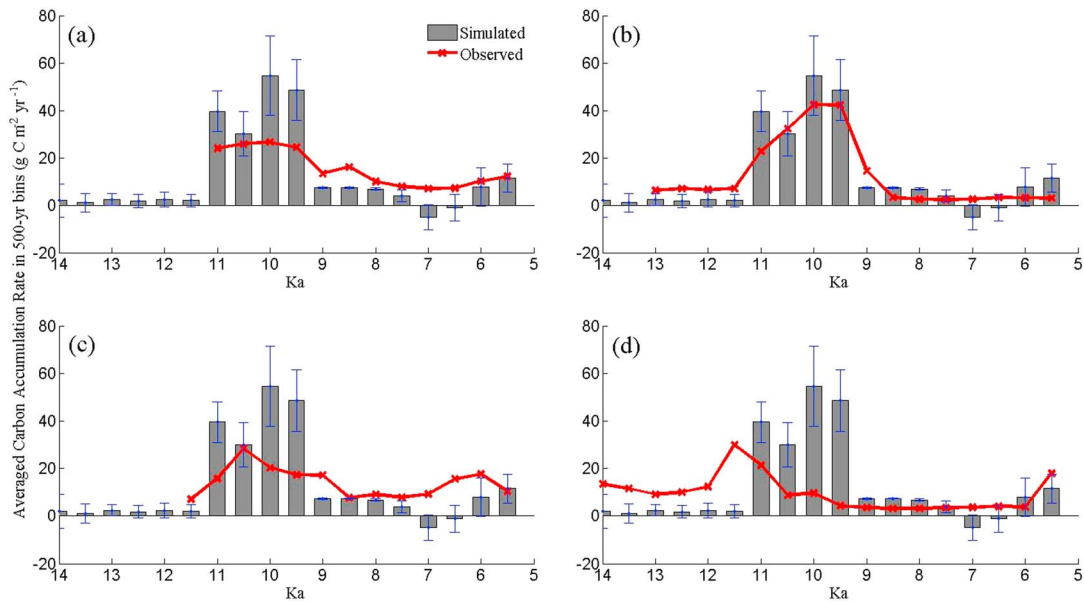


Figure 4. Simulated and observed carbon accumulation rates from 14.5 ka to 5 ka in 500 year bins with standard deviations for (a) No Name Creek, (b) Horse Trail Fen, (c) Kenai Gasfield, and (d) Swanson Fen.

long-term pattern is a large peak of peat carbon accumulation rates at 11 ka–9 ka (HTM) and a secondary peak at 6 ka–5 ka (mid-Holocene). The model captures the largest peak during the HTM at almost all sites, among which the magnitude is accurately estimated at No Name Creek and Horse Trail Fen sites, while there are time shifts and overestimates in magnitude at Kenai Gasfield and Swanson Fen sites. The secondary accumulation peak is captured at No Name Creek, Kenai Gasfield, and Swanson Fen sites, while the model slightly overestimated the rate at mid-Holocene at Horse Trail Fen site. In addition, there is a high-frequency (20 year resolution) variability in magnitude due to changing climate. When the temporal resolution of the results is reduced to 500 year bins (Figure 4), the simulations match the observations well, especially at No Name Creek

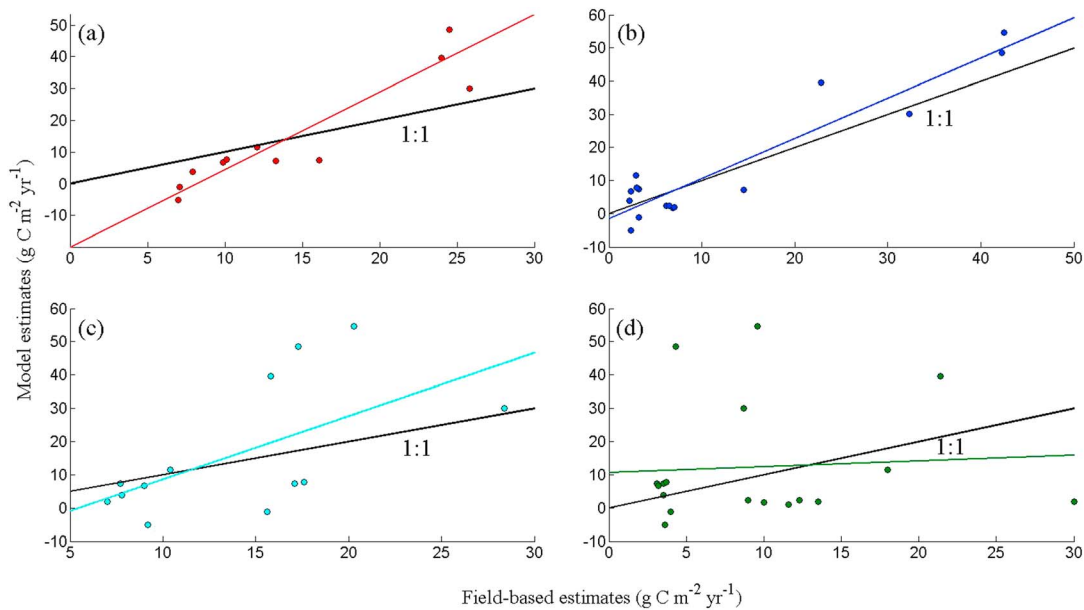


Figure 5. Field-based and model estimates of annual peat carbon accumulation rates in 500 year bins. The linear regressions between simulated and observed estimates are compared with the 1:1 line. For (a) No Name Creek, the linear regression is significant ($P < 0.001$, $N = 12$), with $R^2 = 0.87$, slope = 2.43, and intercept = $-19.85 \text{ g C m}^{-2} \text{ yr}^{-1}$. For (b) Horse Trail Fen, the linear regression is significant ($P < 0.001$, $N = 16$), with $R^2 = 0.88$, slope = 1.21, and intercept = $-1.46 \text{ g C m}^{-2} \text{ yr}^{-1}$. For (c) Kenai Gasfield, the linear regression is significant ($P < 0.001$, $N = 13$), with $R^2 = 0.38$, slope = 1.90, and intercept = $-10.40 \text{ g C m}^{-2} \text{ yr}^{-1}$. For (d) Swanson Fen, the linear regression is significant ($P < 0.001$, $N = 18$), with $R^2 = -0.05$, slope = 0.17, and intercept = $10.69 \text{ g C m}^{-2} \text{ yr}^{-1}$.

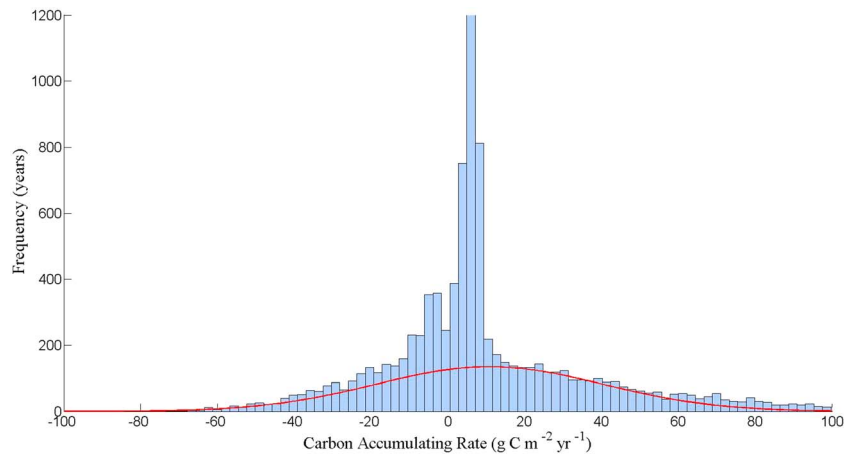


Figure 6. Frequency histogram of simulated peat carbon accumulation rates from 15 ka to 5 ka, characterized with a normal distribution ($\mu = 10.82 \text{ g C m}^{-2} \text{ yr}^{-1}$ and $\sigma = 29.22 \text{ g C m}^{-2} \text{ yr}^{-1}$).

and Horse Trail Fen sites. The simulated trend of carbon accumulation rates is consistent with the synthesis curves from all four sites [Jones and Yu, 2010]. The R^2 coefficient between the simulation and observation are 0.88 for Horse Trail Fen, 0.87 for No Name Creek, 0.38 for Gasfield, and -0.05 for Swanson Fen (Figure 5). The negative correlation at Swanson Fen may be due to the time shift between the simulated accumulation peak in the late HTM and the observed peak in the early HTM. This could be resulted from the dating resolution on the actual cores as more dates (e.g., 20 year bins) would probably shift the peaks in the HTM slightly compared with less dates (e.g., 500 year bins; Figures 3d and 4d).

The frequency distribution of peat carbon accumulation rates over the simulated time period shows a large temporal variability (Figure 6), with a mean rate of $10.82 \text{ g C m}^{-2} \text{ yr}^{-1}$ and standard deviation of $29.22 \text{ g C m}^{-2} \text{ yr}^{-1}$. There is a relatively large proportion of negative accumulation rates, suggesting that a loss of carbon from the soil occurred in some years, especially before the Holocene and in the mid-Holocene (Figure 3). Most rates are within the range of -40 to $40 \text{ g C m}^{-2} \text{ yr}^{-1}$. The rates exceeding $60 \text{ g C m}^{-2} \text{ yr}^{-1}$ occurred mainly during the HTM when there was expansive peatland development. These simulations are consistent with field observations [Yu et al., 2009]. The rates exceeding $15 \text{ g C m}^{-2} \text{ yr}^{-1}$ can be approximated with a normal distribution ($\mu = 10.82 \text{ g C m}^{-2} \text{ yr}^{-1}$ and $\sigma = 29.22 \text{ g C m}^{-2} \text{ yr}^{-1}$). However, the rates smaller than $15 \text{ g C m}^{-2} \text{ yr}^{-1}$ exhibits a nonnormal distribution pattern with a very high frequency from 0 to $15 \text{ g C m}^{-2} \text{ yr}^{-1}$.

Using the observed peat depth bulk density, we estimate the peat depth profile from 15 ka to 5 ka (Figure 7). At No Name Creek, a total depth of 2.5 m is comparable with observed 2.47 m. Although there is a high correlation

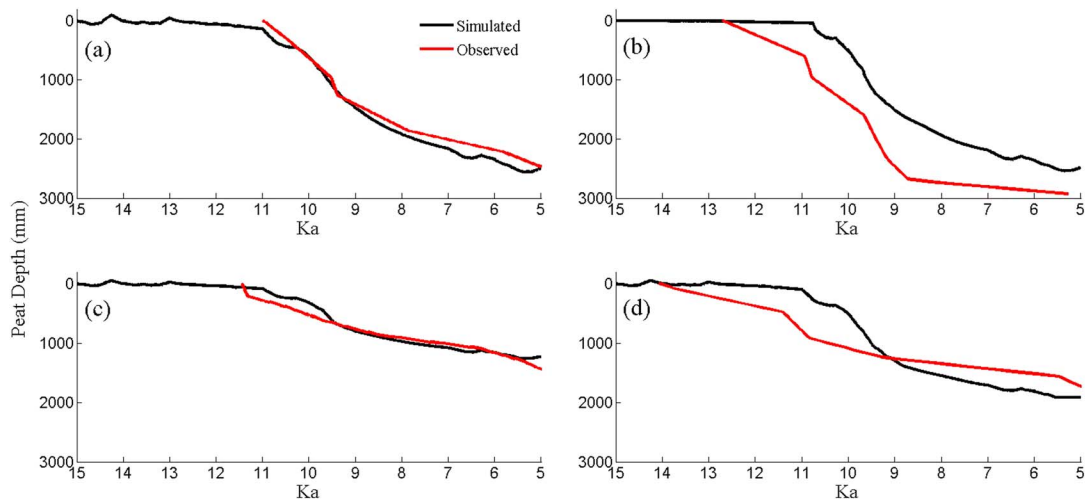


Figure 7. Comparisons between simulated and observed peatland depth profiles: (a) No Name Creek, (b) Horse Trail Fen, (c) Swanson Fen, and (d) Kenai Gasfield.

Table 4. Analysis of Variance Table of the Forward Stepwise Linear Regression Between Carbon Accumulation Rates (Response) and Climate Variables (Predictors)

Variables ^a	F value	R ²
temp	456.14	0.37
NIRR_season	223.86	0.18
temp_season	27.26	0.02
temp × prec	24.93	0.019
prec	8.45	0.007

^aTemperature (temp) and net incoming solar radiation (NIRR) are the annual means, and precipitation (prec) is the annual total. Seasonality of nirr (NIRR_season) and temperature (temp_season) are the annual differences between averages of JJA and DJF.

between simulated and observed peat depths at Horse Trail Fen, the rapid observed carbon accumulation started almost 2000 years before the model estimation. We model a 2.49 m depth versus an observed depth of 2.93 m. The modeled depth profile has a very high correlation with the observation at Kenai Gasfield. The simulated and observed trends stay almost the same with a total depth of 1.2 m and 1.1 m. The observed depth at Swanson Fen

started to increase approximately 3500 years before the model estimation. The total peat depth reaches 1.92 m from simulation compared with 1.76 m from observation. In general, No Name Creek and Kenai Gasfield have the best comparison, while the modeled starting points of peat depth are later than the field estimation at Horse Trail Fen and Swanson Fen sites.

On average, the simulated carbon accumulation rate is $10.82 \text{ g C m}^{-2} \text{ yr}^{-1}$ from 15 ka to 5 ka, while the rate of the HTM is $35.9 \text{ g C m}^{-2} \text{ yr}^{-1}$, which is up to 6 times higher than the rest of the Holocene ($6.5 \text{ g C m}^{-2} \text{ yr}^{-1}$), excluding the rate during the HTM. These are consistent with findings of Jones and Yu [2010], which estimated that the carbon accumulation rate was $\sim 20 \text{ g C m}^{-2} \text{ yr}^{-1}$ from 11.5 ka to 8.6 ka, 4 times higher than the average rate of $\sim 5 \text{ g C m}^{-2} \text{ yr}^{-1}$ over the rest of the Holocene. They found that by 8.6 ka, around 75% of modern Alaskan peatland had formed, followed by a sixfold decrease afterward.

The simulated climate by ECBilt-CLIO shows that, among all time periods, the coolest temperature appeared at 15 ka–13 ka, followed by the mid-Holocene (7 ka–5 ka; Figures 2c and 2d). Those two periods were also generally dry (Figures 2e and 2f). The former represents colder and drier climate before the onset of the HTM [Barber and Finney, 2000; Edwards et al., 2001]. The latter represents post-HTM cooling before the neoglaciation period, which caused permafrost aggradation across northern high latitudes [Oksanen et al., 2001; Zoltai, 1995]. Before the HTM, the mean annual NIRR of the chosen 6 pixels is the lowest among all time periods, approximately 75 W m^{-2} (Figure 2b). Similarly, the mean annual temperature before the HTM for the selected grids is also the lowest among all periods, which is -0.5°C with the lowest mean monthly temperature -10°C and highest 8°C (Figures 2c and 2d). In the early HTM period (11 ka–10 ka), the radiation started to increase and reached 83 W m^{-2} . Meanwhile, the annual temperature increased considerably, reaching 2.36°C . The temperature had its largest increase in summer. The monthly temperature variation suggests that the growing season (monthly temperature above 0°C) had lengthened 10–15 days (Figure 2c). There was also an increase of radiation during the growing season in the early HTM (Figure 2a). We find that the total annual precipitation increased by 75 mm from 510 mm during the early HTM (Figure 2f), with a greater increase in summer than in winter (Figure 2e). It was followed by a wetter-than-before condition in the late HTM (10 ka–9 ka). The solar radiation in growing season continued to increase, reaching the maximum value 87 W m^{-2} at the time, characterized by the highest summer insolation and highest summer temperature as described in Jones and Yu [2010] and Huybers [2006]. Cooler and drier conditions occurred during the mid-Holocene, accompanied by a greater decrease of precipitation in winter than in summer.

The large expansion of Alaskan peatland during the HTM coincides with the maximum summer temperature and NIRR, as well as a wetter-than-before condition. Furthermore, ECBilt-CLIO simulated the increase of temperature and radiation in the growing season, but they remain unchanged in winter among all time periods (Figure 2a). This obviously leads to a stronger seasonality of radiation in the HTM, which has been described in Kaufman et al. [2004, 2016] and Yu et al. [2009]. The rapid peat carbon accumulation in the HTM corresponds to the highest summer temperature along with the highest seasonal radiative forcing. Warmer conditions in summer and the lengthened vegetation growing season, and probably earlier snowmelt during the HTM, positively affect NPP by increasing plant productivity, leading to more carbon input to soils [Running et al., 2004]. Warmer conditions could also lead to a higher decomposition rate of peat SOC [Nobrega and Grogan, 2007;

Dorrepaal *et al.*, 2009]. However, these increases in NPP appear to more than offset warming-induced increases in decomposition.

Hydrological effect can be significant as water table depth could be raised with an increase in precipitation. Higher water tables allow less space for aerobic respiration and give larger space for anaerobic respiration, which reduce the soil carbon loss as aerobic respiration is faster than anaerobic respiration [Hobbie *et al.*, 2000].

A forward stepwise linear regression model between carbon accumulation rates and climate variables was applied. Monthly temperature, monthly NIRR, monthly precipitation, and their seasonalities were put into test. The result suggests that a number of factors are significant ($P < 0.001$; Table 4); temperature has the most significant effect on carbon accumulation rate according to the biggest F value in the analysis of variance table. The seasonality of NIRR also plays an important role, but monthly NIRR, as we thought important above, is not a significant factor. The seasonality of temperature, the interaction of temperature and precipitation, and precipitation alone have relatively minor effects (lower F values) among all significant variables. The seasonality of precipitation is not important. Enhanced temperature, climate seasonality, and enhanced precipitation may help explain the onset of explosive peatland initiation in Alaska during the HTM. The low, even negative carbon accumulation rate during the mid-Holocene is consistent with the unfavorable cool and dry climate conditions. This period experienced lower snowfall than the HTM (Figure 2e). The combination of decreased snowfall and lower temperature (Table 4) resulted in deeper frost depth due to the decreased insulative effects of the snowpack, and therefore shortening the period for active photosynthetic C uptake, leading to an overall low plant productivity [McGuire *et al.*, 2000; Stieglitz *et al.*, 2003].

3.3. Model Sensitivity Analysis

Peat carbon accumulation, water table depth, aerobic respiration in the unsaturated zone, and methane production in the saturated zone are all affected by varying the lowest water table boundary (LWB). In the standard simulation, the mean water table depth is 14 cm below soil surface (Figure S5b), with fluctuation above and below this value. Considering that there is a small change of precipitation among all the time slices (less than 20%), there is no apparent change for the mean water table depth over the simulation period. The simulation under more saturated condition after setting the LWB to 22 cm indicates that mean water table depth increases approximately 5 cm closer to the soil surface, resulting in a slightly increase of aerobic respiration in the unsaturated zone (Figure S5d) and increase of methane production and emission (Figure S5c). Despite the positively affected decomposition, rising water table still resulted in an increase of carbon accumulation rate by up to $40 \text{ g C m}^{-2} \text{ yr}^{-1}$ during the HTM, which may suggest an overwhelming effect of hydrological condition on NPP rather than decomposition. The lower amount of peat SOC in the early Holocene determines the low aerobic respiration (Figure S5a). Respiration subsequently increases coincident with increasing SOC. In contrast, water table drops by 3 cm after setting the LWB to 35 cm, which decreases the carbon accumulation rate by up to $20 \text{ g C m}^{-2} \text{ yr}^{-1}$ in the HTM. An overall methane production rate is simulated at approximately $13 \text{ g C m}^{-2} \text{ yr}^{-1}$ during the HTM. The simulated methane emission is $7 \text{ g C m}^{-2} \text{ yr}^{-1}$, about 60% of the methane production. Assuming that $R_{\text{COM}} : R_{\text{CH}_4}$ is 5, we get the ratio ($\text{CO}_2 : \text{CH}_4$) of the emission rates around 10 under anaerobic conditions after accounting the oxidized CH_4 (~40% of total CH_4 production) for CO_2 release. We estimate that $\sim 78 \text{ g C m}^{-2} \text{ yr}^{-1}$ CO_2 is released via anaerobic respiration, which is ~26% of the aerobic CO_2 production (including CO_2 production from CH_4 oxidation) during the HTM (Figure S5d). This is consistent with observed 24% in Glatzel *et al.* [2004].

At open fen site, when LAI is 0.4, the mean water table depth is at approximately 14 cm (Figure S6b). Under partly forested fen condition with LAI of 2.8, the mean water table depth slightly decreases as the interception of precipitation increases and more water is evaporated. The decreasing water table position enhances aerobic respiration, leading to a slight decrease in peat SOC accumulation over the Holocene (Figures S6a and S6d). In forested peatland with LAI of 5.0, the interception of precipitation continues to increase, making the mean water table depth decrease from 14 cm to 16 cm, resulting in a decrease in peat SOC accumulation. However, the effect of LAI may not be as significant as LWB on the long-term peat SOC accumulation.

4. Conclusions

We develop a peatland ecosystem model to quantify long-term peat carbon accumulation rates in Alaska during the Holocene. The model is evaluated with observational data of soil moisture, water table depth, soil

temperature profile, methane, and carbon fluxes and pools. The model is then applied to four Alaskan peatlands on the Kenai Peninsula. The model estimates well the peat carbon accumulation rate and peat depths throughout the Holocene. The average carbon accumulation rate is $10.82 \text{ g C m}^{-2} \text{ yr}^{-1}$, while the rate of the HTM is $35.9 \text{ g C m}^{-2} \text{ yr}^{-1}$, which is up to 6 times higher than the rest of the Holocene ($6.5 \text{ g C m}^{-2} \text{ yr}^{-1}$). Our simulations are consistent with the observational data. The warming event in the HTM characterized by increased summer temperatures and increased seasonality of solar radiation, along with the wetter-than-before conditions, might have played an important role in determining the carbon accumulation rate. From the sensitivity analysis, we identify that initial water table depth and vegetation canopy are major drivers of carbon accumulation. We plan to use the developed peatland model to quantify regional peat carbon accumulations under changing climate conditions when it is parameterized for various peatland ecosystems.

Acknowledgments

We appreciate the insightful and constructive comments from two anonymous reviewers. We acknowledge the funding support from a NSF project IIS-1027955 and a DOE project DE-SC0008092. We also acknowledge the SPRUCE project to allow us use its data. We also appreciate the comments and suggestions from Paul J. Hanson to this study. Data presented in this paper are publicly accessible: ECBilt-CLIO Paleosimulation (<http://apdrc.soest.hawaii.edu/datadoc/sim2bl.php>) and CRU2.0 (<http://www.cru.uea.ac.uk/data>). Model parameter data and model evaluation process are in Tables S1–S4 and Figures S1–S6 in the supporting information. Other simulation data including model codes are available upon request from the corresponding author (qzhuang@purdue.edu).

References

- Assessment, A. C. I. (2005), Forests, land management and agriculture, *Arctic Clim. Impact Assess.*, 781–862.
- Barber, V. A., and B. P. Finney (2000), Late Quaternary paleoclimatic reconstructions for interior Alaska based on paleolake-level data and hydrologic models, *J. Paleolimnol.*, 24(1), 29–41.
- Bridgman, S. D., J. Pastor, B. Dewey, J. F. Weltzin, and K. Updegraff (2008), Rapid carbon response of peatlands to climate change, *Ecology*, 89(11), 3041–3048.
- Christensen, J. H., and O. B. Christensen (2007), A summary of the PRUDENCE model projections of changes in European climate by the end of this century, *Clim. Change*, 81(1), 7–30.
- Churchill, A. (2011), The response of plant community structure and productivity to changes in hydrology in Alaskan boreal peatlands, Master thesis, 119 pp., Univ. of Alaska, Fairbanks, AK.
- Coughlan, J. C., and S. W. Running (1997), Regional ecosystem simulation: A general model for simulating snow accumulation and melt in mountainous terrain, *Landscape Ecol.*, 12(3), 119–136.
- Conrad, R. (1999), Contribution of hydrogen to methane production and control of hydrogen concentrations in methanogenic soils and sediments, *FEMS Microbiol. Ecol.*, 28(3), 193–202.
- Crill, P. M., et al. (1988), Methane flux from Minnesota peatlands, *Global Biogeochem. Cycles*, 2(4), 371–384, doi:10.1029/GB002i004p00371.
- Davidson, E. A., and I. A. Janssens (2006), Temperature sensitivity of soil carbon decomposition and feedbacks to climate change, *Nature*, 440(7081), 165–173.
- Deng, J., C. Li, and S. Froliking (2015), Modeling impacts of changes in temperature and water table on C gas fluxes in an Alaskan peatland, *J. Geophys. Res.: Biogeosci.*, 120, 1279–1295, doi:10.1002/2014JG002880.
- Dorrepaal, E., S. Toet, R. S. van Logtestijn, E. Swart, M. J. van de Weg, T. V. Callaghan, and R. Aerts (2009), Carbon respiration from subsurface peat accelerated by climate warming in the subarctic, *Nature*, 460(7255), 616–619.
- Edwards, M. E., C. J. Mock, B. P. Finney, V. A. Barber, and P. J. Bartlein (2001), Potential analogues for paleoclimatic variations in eastern interior Alaska during the past 14,000 yr: Atmospheric-circulation controls of regional temperature and moisture responses, *Quat. Sci. Rev.*, 20(1), 189–202.
- Freeman, C., M. A. Lock, and B. Reynolds (1992), Fluxes of CO₂, CH₄ and N₂O from a Welsh peatland following simulation of water table draw-down: Potential feedback to climatic change, *Biogeochemistry*, 19(1), 51–60.
- Froliking, S., N. T. Roulet, E. Tuittila, J. L. Bubier, A. Quillet, J. Talbot, and P. J. H. Richard (2010), A new model of Holocene peatland net primary production, decomposition, water balance, and peat accumulation, *Earth Syst. Dyn.*, 1(1), 1–21.
- Gerdol, R., L. Bragazza, and L. Brancaloni (2008), Heatwave 2003: High summer temperature, rather than experimental fertilization, affects vegetation and CO₂ exchange in an alpine bog, *New Phytol.*, 179(1), 142–154.
- Glatzel, S., N. Basiliko, and T. Moore (2004), Carbon dioxide and methane production potentials of peats from natural, harvested and restored sites, eastern Québec, Canada, *Wetlands*, 261–267.
- Gorham, E. (1991), Northern peatlands: Role in the carbon cycle and probable responses to climatic warming, *Ecol. Appl.*, 1(2), 182–195.
- Gorham, E., J. A. Janssens, and P. H. Glaser (2003), Rates of peat accumulation during the postglacial period in 32 sites from Alaska to Newfoundland, with special emphasis on northern Minnesota, *Can. J. Bot.*, 81(5), 429–438.
- Granberg, G., H. Grip, M. O. Löfvenius, I. Sundh, B. H. Svensson, and M. Nilsson (1999), A simple model for simulation of water content, soil frost, and soil temperatures in boreal mixed mires, *Water Resour. Res.*, 35(12), 3771–3782, doi:10.1029/1999WR900216.
- Hanson, P. J., J. R. Phillips, J. S. Riggs, W. R. Nettles, and D. E. Todd (2014), SPRUCE large-collar in situ CO₂ and CH₄ flux data for the SPRUCE experimental plots. Carbon Dioxide Information Analysis Center, Oak Ridge National Laboratory, U.S. Department of Energy, Oak Ridge, Tenn. [Available at 10.3334/CDIAC/spruce.006.]
- Hanson, P. J., J. S. Riggs, C. Dorrance, W. R. Nettles, and L. A. Hook (2015), SPRUCE environmental monitoring data: 2010–2014 Carbon Dioxide Information Analysis Center, Oak Ridge National Laboratory, U.S. Department of Energy, Oak Ridge, Tenn. [Available at 10.3334/CDIAC/spruce.001.]
- Hay, L. E., R. L. Wilby, and G. H. Leavesley (2000), A comparison of delta change and downscaled GCM scenarios for three mountainous basins in the United States, *J. Am. Water Resour. Assoc.*, 36, 387–397.
- He, Y., M. C. Jones, Q. Zhuang, C. Boicchio, B. S. Felzer, E. Mason, and Z. Yu (2014), Evaluating CO₂ and CH₄ dynamics of Alaskan ecosystems during the Holocene thermal maximum, *Quat. Sci. Rev.*, 86, 63–77.
- Helvey, J. D. (1971), A summary of rainfall interception by certain conifers of North America in *Proceedings of the Third International Symposium for Hydrology Professors Biological Effects in the Hydrological Cycle*, edited by E. J. Monke, 103–113 pp., Purdue Univ., West Lafayette, Ind.
- Hinzman, L. D., L. A. Viereck, P. C. Adams, V. E. Romanovsky, and K. Yoshikawa (2006), Climate and permafrost dynamics of the Alaskan boreal forest, *Alaska's Changing Boreal For.*, 39–61.
- Hobbie, S. E., J. P. Schimel, S. E. Trumbore, and J. R. Randerson (2000), Controls over carbon storage and turnover in high-latitude soils, *Global Change Biol.*, 6(S1), 196–210.
- Huybers, P. (2006), Early Pleistocene glacial cycles and the integrated summer insolation forcing, *Science*, 313(5786), 508–511.

- Iversen, C. M., P. J. Hanson, D. J. Brice, J. R. Phillips, K. J. McFarlane, E. A. Hobbie, and R. K. Kolka (2014), SPRUCE peat physical and chemical characteristics from experimental plot cores, 2012 Carbon Dioxide Information Analysis Center, Oak Ridge National Laboratory, U.S. Department of Energy, Oak Ridge, Tenn. [Available at 10.3334/CDIAC/spruce.005.]
- Jones, M. C., and Z. Yu (2010), Rapid deglacial and early Holocene expansion of peatlands in Alaska, *Proc. Natl. Acad. Sci.*, 107(16), 7347–7352.
- Kaufman, D. S., et al. (2004), Holocene thermal maximum in the western Arctic (0–180°W), *Quat. Sci. Rev.*, 23, 529–560.
- Kaufman, D. S., et al. (2016), Holocene climate changes in eastern Beringia (NW North America)—A systemic review of multi-proxy evidence, *Quat. Sci. Rev.*, doi:10.1016/j.quascirev.2015.10.021.
- Keller, J. K., and S. D. Bridgman (2007), Pathways of anaerobic carbon cycling across an ombrotrophic–minerotrophic peatland gradient, *Limnol. Oceanogr.*, 52, 96–107.
- Keller, J. K., and K. K. Takagi (2013), Solid-phase organic matter reduction regulates anaerobic decomposition in bog soil, *Ecosphere*, 4(5), 1–12.
- Kirschbaum, M. U. (1993), A modelling study of the effects of changes in atmospheric CO₂ concentration, temperature and atmospheric nitrogen input on soil organic carbon storage, *Tellus B*, 45(4), 321–334.
- Kirschbaum, M. U. (1995), The temperature dependence of soil organic matter decomposition, and the effect of global warming on soil organic C storage, *Soil Biol. Biochem.*, 27(6), 753–760.
- Kirschbaum, M. U. (2000), Will changes in soil organic carbon act as a positive or negative feedback on global warming?, *Biogeochemistry*, 48(1), 21–51.
- Kirschbaum, M. U. F. (2006), The temperature dependence of organic-matter decomposition—Still a topic of debate, *Soil Biol. Biochem.*, 38(9), 2510–2518.
- Knorr, W., I. C. Prentice, J. I. House, and E. A. Holland (2005), Long-term sensitivity of soil carbon turnover to warming, *Nature*, 433(7023), 298–301.
- Lappalainen, E. (Ed) (1996), *Global Peat Resources*, vol. 4, International Peat Society, Jyväskylä.
- Loisel, J., et al. (2014), A database and synthesis of northern peatland soil properties and Holocene carbon and nitrogen accumulation, *The Holocene*, doi:10.1177/0959683614538073.
- McGuire, A. D., J. M. Melillo, D. W. Kicklighter, and L. A. Joyce (1995), Equilibrium responses of soil carbon to climate change: Empirical and process-based estimates, *J. Biogeography*, 785–796.
- McGuire, A. D., and J. E. Hobbie (1997), Global climate change and the equilibrium responses of carbon storage in arctic and subarctic regions, in *Modeling the Arctic System: A Workshop Report on the State of Modeling in the Arctic System Science Program*, pp. 53–54, Arctic Research Consortium of the U.S., Fairbanks, Alaska.
- McGuire, A. D. et al. (2000), Modeling the effects of snowpack on heterotrophic respiration across northern temperate and high latitude regions: Comparison with measurements of atmospheric carbon dioxide in high latitudes, *Biogeochemistry*, 48(1), 91–114.
- McGuire, A. D., et al. (2009), Sensitivity of the carbon cycle in the Arctic to climate change, *Ecol. Monogr.*, 79(4), 523–555.
- Moore, T. R., and R. Knowles (1989), The influence of water table levels on methane and carbon dioxide emissions from peatland soils, *Can. J. Soil Sci.*, 69(1), 33–38.
- Nobrega, S., and P. Grogan (2007), Deeper snow enhances winter respiration from both plant-associated and bulk soil carbon pools in birch hummock tundra, *Ecosystems*, 10(3), 419–431.
- Oksanen, P. O., P. Kuhry, and R. N. Alekseeva (2001), Holocene development of the Rogovaya river peat plateau, European Russian Arctic, *The Holocene*, 11(1), 25–40.
- Post, W. M., W. R. Emanuel, P. J. Zinke, and A. G. Stangenberger (1982), Soil carbon pools and world life zones, *Nature*, 298, 156–159.
- Renssen, H., H. Seppä, O. Heiri, D. M. Roche, H. Goosse, and T. Fichefet (2009), The spatial and temporal complexity of the Holocene thermal maximum, *Nat. Geosci.*, 2(6), 411–414.
- Roulet, N. T., P. M. Lafleur, P. J. Richard, T. R. Moore, E. R. Humphreys, and J. I. L. L. Bubier (2007), Contemporary carbon balance and late Holocene carbon accumulation in a northern peatland, *Global Change Biol.*, 13(2), 397–411.
- Running, S. W., R. R. Nemani, F. A. Heinsch, M. Zhao, M. Reeves, and H. Hashimoto (2004), A continuous satellite-derived measure of global terrestrial primary production, *BioScience*, 54, 547–560.
- Senkowsky, S. (2001), A burning interest in boreal forests: Researchers in Alaska link fires with climate change, *BioScience*, 51(11), 916–921.
- Spahni, R., F. Joos, B. D. Stocker, M. Steinacher, and Z. C. Yu (2013), Transient simulations of the carbon and nitrogen dynamics in northern peatlands: From the Last Glacial Maximum to the 21st century, *Clim. Past*, 9(3), 1287–1308.
- Stieglitz, M., S. J. Déry, V. E. Romanovsky, and T. E. Osterkamp (2003), The role of snow cover in the warming of arctic permafrost, *Geophys. Res. Lett.*, 30(13), 1721, doi:10.1029/2003GL017337.
- Tang, J., Q. Zhuang, R. D. Shannon, and J. R. White (2010), Quantifying wetland methane emissions with process-based models of different complexities, *Biogeosciences*, 7(11), 3817–3837.
- Timm, O., and A. Timmermann (2007), Simulation of the last 21,000 years using accelerated transient boundary conditions*, *J. Clim.*, 20(17), 4377–4401.
- Turetsky, M. R., C. C. Treat, M. P. Waldrop, J. M. Waddington, J. W. Harden, and A. D. McGuire (2008), Short-term response of methane fluxes and methanogen activity to water table and soil warming manipulations in an Alaskan peatland, *J. Geophys. Res.*, 113, G00A10, doi:10.1029/2007JG000496.
- Turetsky, M. R., et al. (2014), A synthesis of methane emissions from 71 northern, temperate, and subtropical wetlands, *Global Change Biol.*, 20(7), 2183–2197.
- Turunen, J., E. Tomppo, K. Tolonen, and A. Reinikainen (2002), Estimating carbon accumulation rates of undrained mires in Finland—Application to boreal and subarctic regions, *The Holocene*, 12(1), 69–80.
- Wang, Y. P., and P. J. Polglase (1995), Carbon balance in the tundra, boreal forest and humid tropical forest during climate change: Scaling up from leaf physiology and soil carbon dynamics, *Plant, Cell & Environ.*, 18(10), 1226–1244.
- Yavitt, J. B., G. E. Lang, and R. K. Wieder (1987), Control of carbon mineralization to CH₄ and CO₂ in anaerobic, *Sphagnum*-derived peat from Big Run Bog, West Virginia, *Biogeochemistry*, 4(2), 141–157.
- Yu, Z., D. W. Beilman, and M. C. Jones (2009), Sensitivity of northern peatland carbon dynamics to Holocene climate change, *Carbon Cycling Northern Peatlands*, 55–69.
- Yu, Z., J. Loisel, D. P. Brosseau, D. W. Beilman, and S. J. Hunt (2010), Global peatland dynamics since the Last Glacial Maximum, *Geophys. Res. Lett.*, 37, L13402, doi:10.1029/2010GL043584.
- Zhuang, Q., V. E. Romanovsky, and A. D. McGuire (2001), Incorporation of a permafrost model into a large-scale ecosystem model: Evaluation of temporal and spatial scaling issues in simulating soil thermal dynamics, *J. Geophys. Res.*, 106(D24), 33,649–33,670, doi:10.1029/2001JD900151.
- Zhuang, Q., A. D. McGuire, K. P. O'Neill, J. W. Harden, V. E. Romanovsky, and J. Yarie (2002), Modeling soil thermal and carbon dynamics of a fire chronosequence in interior Alaska, *J. Geophys. Res.*, 107(D1), 8147, doi:10.1029/2001JD001244.

- Zhuang, Q., et al. (2003), Carbon cycling in extratropical terrestrial ecosystems of the Northern Hemisphere during the 20th century: A modeling analysis of the influences of soil thermal dynamics, *Tellus B*, 55(3), 751–776.
- Zhuang, Q., et al. (2004), Methane fluxes between terrestrial ecosystems and the atmosphere at northern high latitudes during the past century: A retrospective analysis with a process-based biogeochemistry model, *Global Biogeochem. Cycles*, 18, GB3010, doi:10.1029/2004GB002239.
- Zhuang, Q., et al. (2006), CO₂ and CH₄ exchanges between land ecosystems and the atmosphere in northern high latitudes over the 21st century, *Geophys. Res. Lett.*, 33, L17403, doi:10.1029/2006GL026972.
- Zhuang, Q., et al. (2015), Influence of changes in wetland inundation extent on net fluxes of carbon dioxide and methane in northern high latitudes from 1993 to 2004, *Environ. Res. Lett.*, 10, 095009.
- Zoltai, S. C. (1995), Permafrost distribution in peatlands of west-central Canada during the Holocene warm period 6000 years BP, *Géogr. Phys. et Quat.*, 49(1), 45–54.